Association of Antarctic polar stratospheric cloud formation on tropospheric cloud systems

Zhien Wang,[1] Graeme Stephens,[2] Terry Deshler,[1] Charles Trepte,[3] Thomas Parish,[1] Deborah Vane,[4] Dave Winker,[3] Dong Liu,[1] and Loknath Adhikari[1]

Received 2 April 2008; revised 22 May 2008; accepted 2 June 2008; published 4 July 2008.

[1] The formation of polar stratospheric clouds (PSCs) is critical to the development of polar ozone loss. However, the mechanisms of PSC formation remain poorly understood, which affects ozone loss models. Here, based on observations by the NASA A-train satellites, we show that 66% ± 16% and 52% ± 17% of PSCs over west and east Antarctica during the period June–October 2006 were associated with deep tropospheric cloud systems, with maximum depths exceeding 7 km. The development of such deep tropospheric cloud systems should cool the lower stratosphere through adiabatic and radiative processes, favoring PSC development. These deep systems also transport lower tropospheric air into the upper troposphere and lower stratosphere. These new findings suggest that Antarctic PSC formation is closely connected to tropospheric meteorology and thus governed by synoptic scale dynamics, local topography, and large-scale circulation. More dedicated studies are still needed to better understand Antarctic PSC formation. **Citation:** Wang, Z., G. Stephens, T. Deshler, C. Trepte, T. Parish, D. Vane, D. Winker, D. Liu, and L. Adhikari (2008), Association of Antarctic polar stratospheric cloud formation on tropospheric cloud systems, *Geophys. Res. Lett.*, *35*, L13806, doi:10.1029/2008GL034209.

1. Introduction

[2] The formation of polar stratospheric clouds (PSCs) is critical to the development of polar ozone loss. Inactive chlorine species are converted into reactive chlorine species on the surfaces of PSC particles [*Solomon*, 1999]. PSCs form when temperatures are cold enough for the low abundance of stratospheric water and nitric acid vapors to condense on pre-existing stratospheric aerosol. In the winter, the Antarctic stratosphere is strongly controlled by a polar vortex [*World Meteorological Organization* (*WMO*), 2007], which inhibits strong mixing with the low-latitude stratosphere, resulting in a cold environment and in the isolation of stratospheric gases and aerosol. Tropospheric synoptic or mesoscale events enhance local cooling in the low stratosphere, which should also enhance PSC formation in the lower stratosphere [*Cariolle et al.*, 1989; *Carslaw et al.*, 1998; *Teitelbaum et al.*, 2001]; however, it is not clear to what extent tropospheric meteorology contributes to Antarctic PSC formation in general. Deep tropospheric cloud systems are normally associated with large-scale lifting or strong local convective and cyclonic activities. The existence of deep tropospheric cloud systems is a good indicator of tropospheric upwelling. Correlations between PSCs and tropospheric cloud systems suggest that tropospheric dynamics may play a significant role in PSC formation.

[3] Our present understanding of PSCs is based on extensive laboratory investigations [e.g. *Hanson and Mauersberger*, 1988], measurements carried out in situ [e.g. *Carslaw et al.*, 1994; *Fahey et al.*, 2001], by remote sensing [e.g. *Santacesaria et al.*, 2001; *Fromm et al.*, 2003], and modeling studies. Remote sensing observations bring a global perspective to our understanding, and allowing integration of the data into global models. Due to cold surface temperatures over Antarctica, it has been difficult to differentiate tropospheric cloudiness from the surface in previous nadir viewing passive satellite measurements. Recent space-based lidar measurements [*Palm et al.*, 2005; *Winker et al.*, 2007], particularly those from the CALIPSO satellite have been combined with the cloud radar observations of CloudSat flying along the same trajectory with a lag of less than 20 seconds [*Stephens et al.*, 2002]. These combined data provide the first real view of tropospheric cloudiness and PSC distribution during winter in Antarctica.

2. Data Analysis

[4] We used CloudSat and CALIPSO data from June–October 2006 to explore the connection between PSCs and tropospheric cloud systems. We used the combined data to determine the cloud distribution over Antarctica. The CloudSat GEOPROF product was used to provide cloudy bins (cloud mask value of $\geq$30) from radar measurements [*Marchand et al.*, 2008], while CALIPSO Level 1B data were averaged to the CloudSat horizontal resolution ($\sim$1.1 km) with 180 m vertical resolution and collocated with CloudSat data for cloud detection using the Attenuated Lidar Scattering Ratio (ALSR). ALSR is the ratio of total signal to molecular-only signal, which is estimated from CALIPSO measurements during cloud-free periods. The following approach is applied to day and night time ALSR profiles between −60 to −90 S to detect tropospheric clouds. For each profile, the first layer cloud base was defined as the first bin with ALSR > 3.5 above the surface, and the first layer top as where the ALSR first dipped below 2. The second and higher cloud layers were searched

[1]Department of Atmospheric Science, University of Wyoming, Laramie, Wyoming, USA.
[2]Department of Atmospheric Science, Colorado State University, Fort Collins, Colorado, USA.
[3]NASA Langley Research Center, Hampton, Virginia, USA.
[4]Jet Propulsion Laboratory, Pasadena, California, USA.

0094-8276/08/2008GL034209$05.00

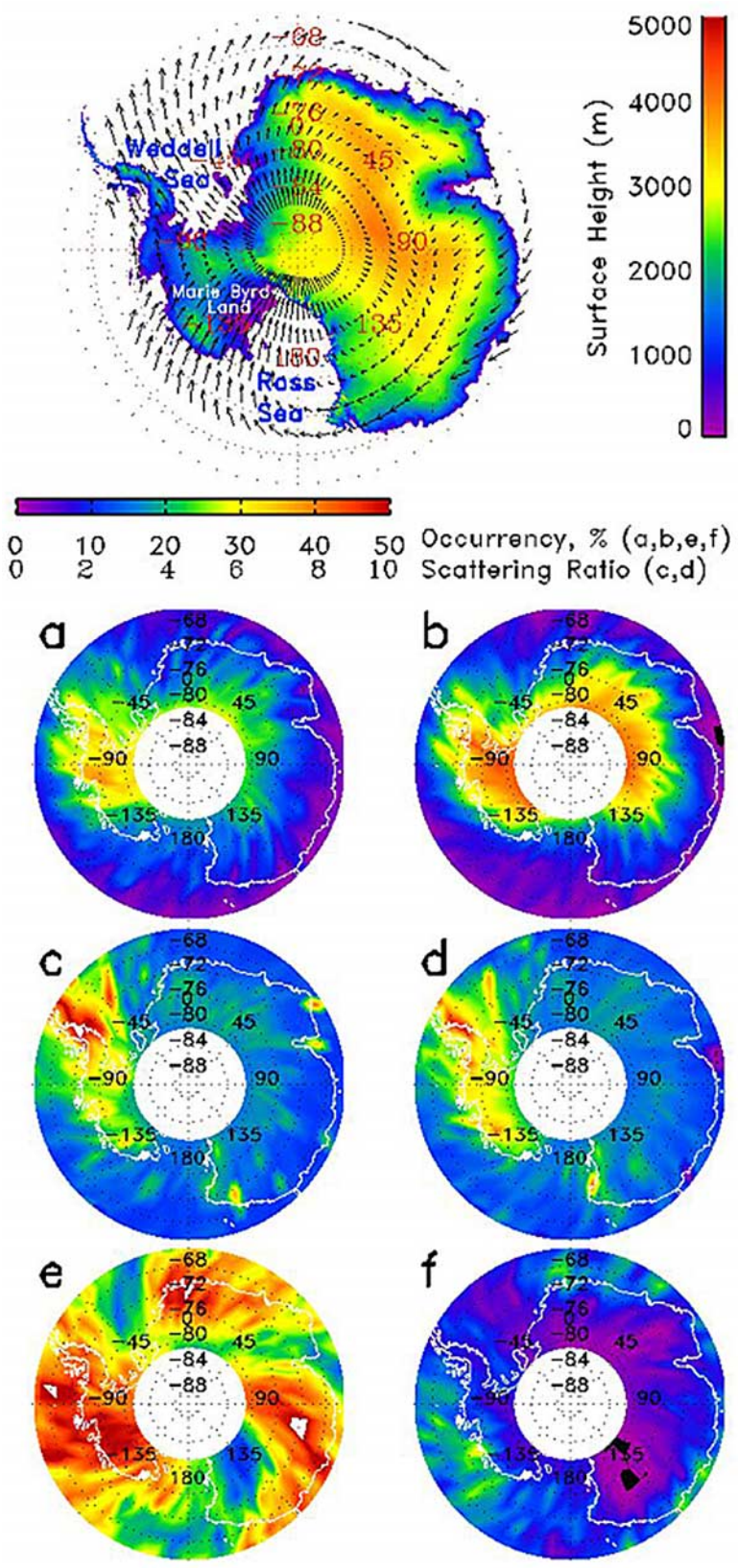

Figure 1. PSC and tropospheric cloud distributions between June and October 2006 observed by CloudSat and CALIPSO. (a) PSC occurrences for heights between 20–25 km, (b) PSC occurrences for heights between 15–20 km, (c) mean ALSRs for heights between 20–25 km, (d) mean ALSRs for heights between 15–20 km, (e) occurrence of tropospheric clouds higher than 7.5 km, and (f) occurrence of tropospheric clouds deeper than 7 km. All results are calculated in a 2.5° × 5° grid (latitude and longitude). The top plot shows the Antarctic surface height map plotted with 200 hPa mean winds from NCEP reanalysis during this period.

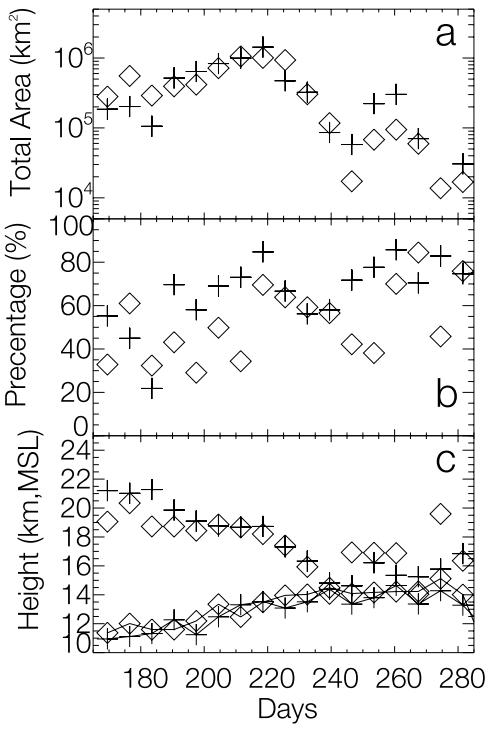

Figure 2. (a) Weekly PSC areas in the vertical cross-section under satellite tracks, (b) percentage of PSCs (in area) associated with tropospheric cloud systems with a maximum depth greater than 7 km, and (c) mean PSC base height (symbols only) with mean maximum cloud top height (symbols connected by a line). Pluses and diamonds represent west and east Antarctica, respectively.

upward in a similar fashion. For cases where there was no gap between PSC and the tropospheric cloud system, the tropospheric cloud top was determined at a level where ALSR decreased below 4 and the ALSR at ~900 m below >8. The CALIPSO cloud base and top heights were limited below 12 and 15 km, MSL (Mean Sea Level), respectively. This simple approach ignores some optically thin clouds, which are not important for this study because of their weak impacts on the stratosphere. After cloudy bins were identified from the collocated CALIPSO and CloudSat measurements, they were merged to provide the vertical structures of tropospheric clouds at the CloudSat vertical resolution (240 m) for further analysis [*Wang and Sassen*, 2001].

[5] A similar method described by *Pitts et al.* [2007] is used for detecting PSC with a slightly higher threshold. First, CALIPSO data is moving-averaged to 20 km horizontally to improve the signal-to-noise ratio for ALSR calculation in the stratosphere. For night time, vertical bins above 12 km and the tropospheric cloud top with ALSR > 1.8 are defined as PSC. In the daytime, depending on the solar background and height, the thresholds are increased to exclude solar noise.

[6] To understand the extent to which Antarctic PSCs are associated with tropospheric cloud systems, vertically and horizontally connected tropospheric cloud or PSC bins were grouped together as tropospheric cloud or PSC systems. To further reduce false PSC detections caused by solar noise, we calculated the areas of PSC systems. PSC systems smaller than 100 bins during the daytime were considered noises. The PSC detection results were also visually inspected for quality control.

3. Results and Discussion

[7] Although PSCs exist almost everywhere, seasonally-averaged map indicates two main regions with high PSC occurrence (Figures 1a and 1b): 1) Marie Byrd Land and the Antarctic Peninsula, and 2) the southern side of East Antarctica. The contrast between these two areas is reflected in their mean ALSRs (Figures 1c and 1d). Over Marie Byrd Land, and especially over the Antarctic Peninsula, the mean PSC scattering ratio is significantly higher than over the other regions.

[8] Topographically-forced mountain waves have been regarded as one of important Antarctic PSC formation mechanisms. PSCs formed under mountain waves tend to be localized along the coast of Antarctica, and they tend to remain quasi-stationary relative to the mean stratospheric flow [*Cariolle et al.*, 1989]. Thus, the observed PSC distribution pattern cannot be explained by mountain wave effect. Synoptic- and meso-scale cyclonic activities are very common over west Antarctica. The Ross Sea/Ross Ice Shelf region, the northern part of the Antarctic Peninsula, and the southern part of the Weddell Sea are the regions most active in mesoscale cyclogenesis [*Simmonds and Keay*, 2000; *Carrasco et al.*, 2003]. Intense cyclonic activity disturbs the upper troposphere and causes quasi-adiabatic uplift through the lower stratosphere, in some cases, cooling the air sufficiently to form PSCs. This dynamic perturbation has been identified as an important PSC formation mechanism over the arctic [*Teitelbaum et al.*, 2001]. For predominantly westerly flow in the upper troposphere and lower stratosphere, it is reasonable to expect high PSC occurrence downwind of regions of mesoscale cyclogenesis, assuming cyclonic activity is a mechanism for PSC formation over Antarctica. Intense cyclones are also typically accompanied by the development of deep tropospheric cloud systems. Under these circumstances, a strong correlation between PSCs and deep tropospheric cloud systems (including deep clouds and extended middle and high clouds) is expected. The map of occurrence of high clouds (Figure 1e) shows that high clouds are observed over the downwind areas of the regions of mesoscale cyclogenesis. As indicated in Figure 1f, deep clouds form mainly along the shore, but high clouds associated with these deep clouds can extend deep into Antarctica and cover a larger area. High PSC occurrence areas (Figures 1a and 1b) appear embedded in regions of high cloud occurrence (Figure 1e).

[9] When tropospheric cloud systems with cloud maximum depths exceeding 7 km are observed beneath a PSC system, the PSC system is considered to be associated with the tropospheric cloud system. Weekly averages of PSC area, cloud height, and cloud system association fraction are shown in Figure 2. The total vertical area of PSCs (Figure 2a) along the CloudSat orbit slowly increases with small week-to-week variation, until a significant decrease begins around mid-August. Figure 2b shows that 66 ± 16% and 52 ± 17% PSCs are directly associated with deep tropospheric cloud systems over west and east Antarctica, respectively, although it should be noted that these percentages change

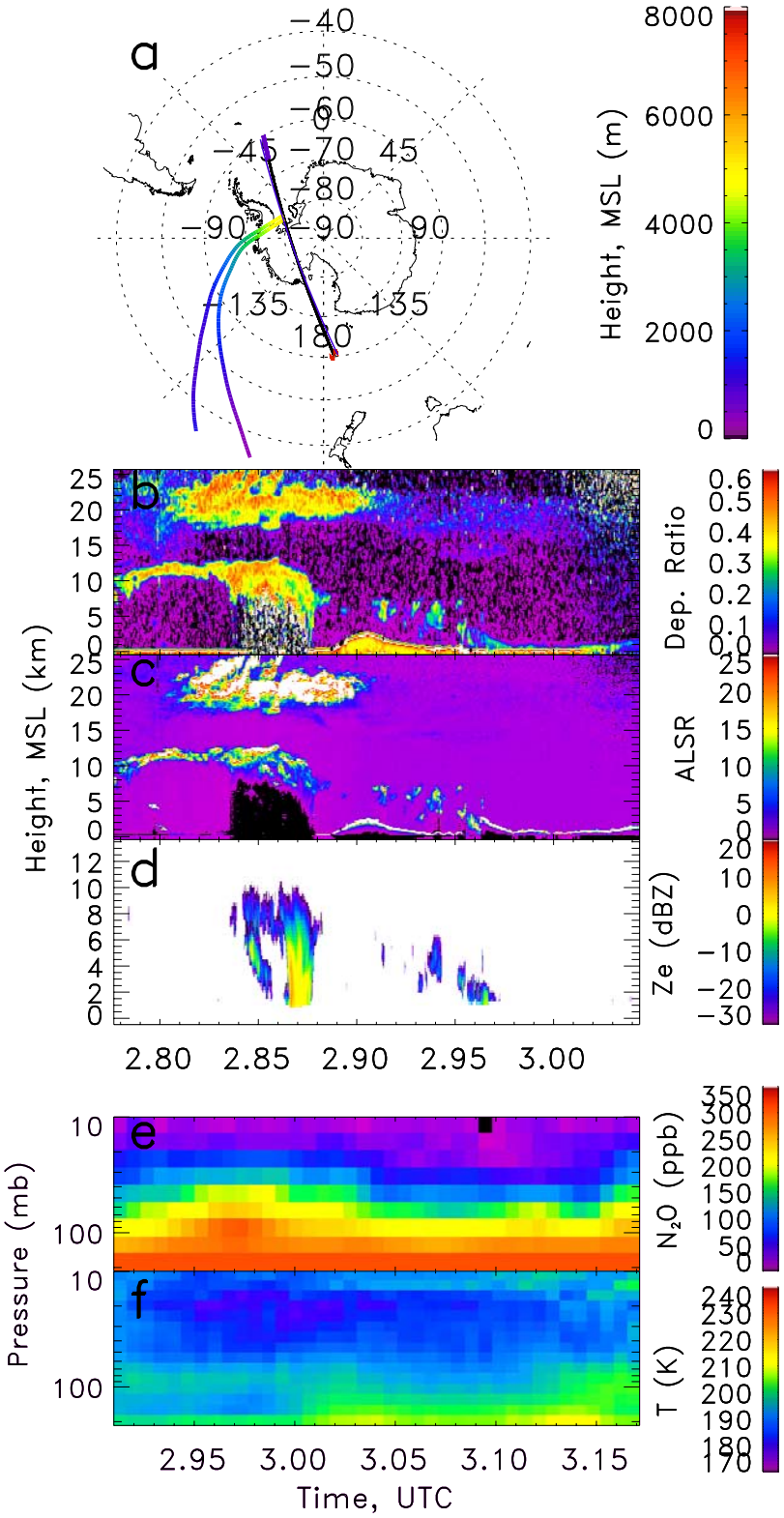

Figure 3. Observations on July 25, 2006. (a) Satellite tracks (black lines), with red end indicating the right sides of the time-height plots in the other plots. Color lines show the height evolutions of 4-day back trajectories (based on the NOAA HYSPLIT model using the vertical velocity of global reanalysis data) for air parcels at 5 km at two locations where deep clouds were observed by CloudSat radar. CALIPSO 532 nm lidar (b) depolarization ratio and (c) ALSR collocated with (d) CloudSat Radar reflectivity (Z_e), (e) Aura MLS N_2O, and (f) temperature.

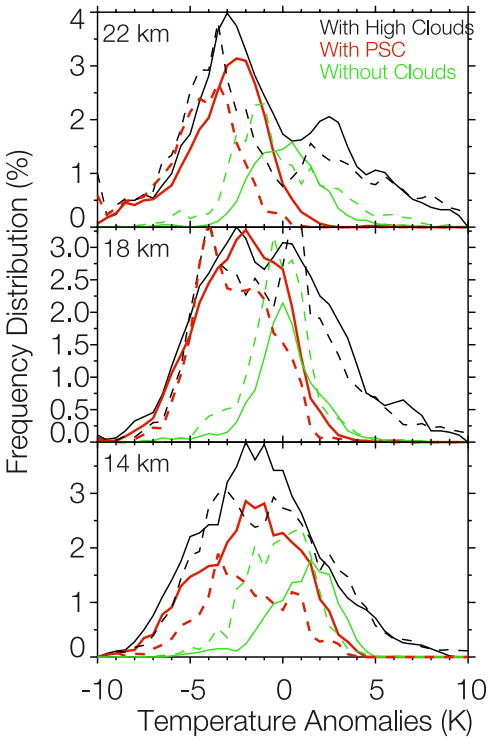

Figure 4. Distribution of low stratospheric temperature anomalies over 70–120°W and 65–80°S associated with PSCs, clouds above 7.5 km, or cloud-free conditions. Solid lines are from MLS temperature retrievals and dashed lines are from ECMWF forecast results. Temperature anomalies are calculated relative to the means of 2.5° × 5° grids.

with time. Before mid-August, the fraction of cloud association is approximately 50%. The increasing percentage of cloud association as winter progresses indicates the increasing importance of tropospheric cloudiness on PSC formation over Antarctica. Following the sharp decrease of PSC amounts in late August (around day 240), a second maximum occurs in mid- and late September, which correlates with a high percentage of cloud association. During this period, solar radiation returns to Antarctica and stratosphere ozone loss begins. The further southern penetrations of weather systems over west Antarctica certainly contribute to the stronger association of PSCs with tropospheric cloud systems over west Antarctica than east Antarctica, but the complex interactions of dynamics and terrain must be further explored.

[10] The development of deep tropospheric cloud systems may affect PSC formation because of their ability to cool the lower stratosphere radiatively and adiabatically. Deep tropospheric cloud systems over Antarctica develop mainly along frontal systems embedded in regions of cyclonic activity. These meteorological conditions produce synoptic-scale and mesoscale uplift to the lower stratosphere [*Teitelbaum et al.*, 2001]. The additional adiabatic cooling of air above the clouds provides conditions favorable for PSC formation, especially during September and October when PSC formation requires lower temperatures due to lower H_2O and HNO_3 gas concentrations caused by the dehydration and denitrification processes associated with PSC formation in early winter. An example of a deep cloud system linked to a PSC system in the Weddell Sea is shown in Figure 3. Although the deep part of clouds extends only ~200 km horizontally, as indicated by CloudSat radar measurements, the optically thick upper tropospheric clouds extend over much larger areas, as indicated by CALIPSO measurements. MLS measurements on Aura indicate cooling below 190 K between 8 and 30 hPa above the tropospheric cloud system. Optically thick PSCs were observed in this region by lidar (Figures 3b and 3c). In contrast, only optically thin PSCs formed at the same altitudes in regions lacking tropospheric clouds beneath.

[11] The colder upper tropospheric clouds reduce upwelling long wave radiation, thereby enhancing radiative cooling of the stratosphere. Radiative calculations based on ozone and temperature sonde data collected in August 2006 at McMurdo Station indicate that clouds with an ice water path of 20 g/m^2 at 10–12 km can produce an additional 0.1 K/day of cooling in the lower stratosphere. This additional cooling, compared to clear-sky cooling, is significant when it occurs between 15 and 20 km. Although radiative cooling is small compared to adiabatic cooling, its importance emerges for persistent cloud systems and for supplying adiabatic cooling. Temperature anomalies over 70–120°W and 65–80°S at three different altitudes (Figure 4), estimated based on MLS satellite measurements and ECMWF model analysis, clearly indicate that both PSCs and high clouds are associated with low stratospheric temperatures slightly colder than the average.

[12] Deep tropospheric cloud development is often associated with strong vertical transport, which brings lower tropospheric air (trace gases and aerosols) into the upper troposphere and possibly lower stratosphere. Back trajectories indicate that air parcels at 5 km in deep clouds observed over the Weddell Sea (Figure 3a) originate at mid-latitudes, about four days earlier, within a layer extending from the near surface to an altitude of approximately 2000 m. N_2O profiles from MLS (Figure 3e) suggest that tropospheric air reaches as high as 60 hPa (~17 km) in the area of cloud system development. Gravity waves generated above tropospheric clouds can also generate a mixing layer characterized by weak vertical gradients of potential temperature and other tracers in the upper troposphere and lower stratosphere. Thus, uplifted tropospheric air may spread into a larger area in the lower stratosphere through isentropic mixing, mixing associated with gravity waves, or other tropopause disturbances. The addition of tropospheric air to the stratosphere may affect stratospheric chemistry.

[13] In general, PSC base height (Figure 2c) decreases with time, and this may be caused by diabatic descent of air in the polar vortex, together with dehydration and denitrification processes [*Rosenfield et al.*, 1994; *WMO*, 2007]. Meanwhile, the weekly mean of maximum cloud top height increases with time until the end of September, when the stratosphere begins to warm. During late August and throughout September, most PSCs are connected to deep tropospheric clouds. The changes in the distance between PSC base height and tropospheric cloud top height suggest that tropospheric cloud systems may play different roles in PSC formation at different time periods. Before mid-August, cloud systems mainly provide additional cooling for the lower stratosphere; however, the close connection between

PSCs and cloud systems in the later PSC formation period indicates possible transport of tropospheric air into the lower stratosphere, enhancing PSC formation. The late winter Antarctic tropopause is essentially non-existent and significant vertical coupling between the troposphere and stratosphere is likely.

[14] Although the results here illustrate that Antarctic PSC formation is strongly associated with tropospheric synoptic and mesoscale conditions, it is unclear how complex interactions of air flows of different scales in the troposphere and potential climate changes will affect Antarctic PSC formations. The topographic inhomogeneity over Antarctica produces a strong katabatic wind regime [*Parish*, 1992] that has been linked to mesoscale cyclogenesis over Antarctica [*Carrasco et al.*, 2003]. Mesoscale cyclones also strongly interact with synoptic and larger-scale conditions and the complex terrain [*Carrasco et al.*, 2003]. Climate model simulations indicate that climate change could result in stronger storms in the polar region [*Yin*, 2005]. Thus, predicting year-to-year variations of the Antarctic ozone hole may require a deeper understanding of Antarctic tropospheric disturbances and further detailed studies are needed.

[15] **Acknowledgments.** This research was supported by the NASA CloudSat and CALIPSO projects.

References

Cariolle, D., S. Muller, and F. Cayla (1989), Mountain waves, stratospheric clouds, and the ozone depletion over Antarctica, *J. Geophys. Res.*, *94*, 11,233–11,240.

Carrasco, J. F., D. H. Bromwich, and A. J. Monaghan (2003), Distribution and characteristics of mesoscale cyclones in the Antarctic: Ross Sea eastward to the Weddell Sea, *Mon. Weather Rev.*, *131*, 289–301.

Carslaw, K. S., B. P. Luo, S. L. Clegg, T. Peter, P. Brimblecombe, and P. J. Crutzen (1994), Stratospheric aerosol growth and HNO_3 gas phase depletion from coupled HNO_3 and water uptake by liquid particles, *Geophys. Res. Lett.*, *21*, 2479–2482.

Carslaw, K. S., et al. (1998), Increased stratospheric ozone depletion due to mountain-induced atmospheric waves, *Nature*, *391*, 675–678.

Fahey, D. W., et al. (2001), The detection of large HNO_3-containing particles in the winter Arctic stratosphere, *Science*, *291*, 1026–1031.

Fromm, M., J. Alfred, and M. Pitts (2003), A unified, long-term, high-latitude stratospheric aerosol and cloud database using SAM II, SAGE II, and POAM II/III data: Algorithm description, database definition, and climatology, *J. Geophys. Res.*, *108*(D12), 4366, doi:10.1029/2002JD002772.

Hanson, D. R., and K. Mauersberger (1988), Laboratory studies of the nitric acid trihydrate: Implication for the south polar stratosphere, *Geophys. Res. Lett.*, *15*, 855–858.

Marchand, R., G. G. Mace, T. Ackerman, and G. Stephens (2008), Hydrometeor detection using CloudSat—An Earth-orbiting 94-GHz cloud radar, *J. Atmos. Oceanic Technol.*, *25*, 519–533.

Parish, T. R. (1992), On the role of Antarctic katabatic winds in forcing large-scale tropospheric motions, *J. Atmos. Sci.*, *49*, 1374–1385.

Palm, S. P., M. Fromm, and J. Spinhirne (2005), Observations of Antarctic polar stratospheric clouds by the Geoscience Laser Altimeter System (GLAS), *Geophys. Res. Lett.*, *32*, L22S04, doi:10.1029/2005GL023524.

Pitts, M. C., L. W. Thomason, L. R. Poole, and D. M. Winker (2007), Characterization of polar stratospheric clouds with space-borne lidar: CALIPSO and the 2006 Antarctic season, *Atmos. Chem. Phys.*, *7*, 5207–5228.

Rosenfield, J. E., P. A. Newman, and M. R. Schoeberl (1994), Computations of diabatic decent in the stratospheric polar vortex, *J. Geophys. Res.*, *99*, 16,677–16,689.

Santacesaria, V., A. R. MacKenzie, and L. Stefanutti (2001), A climatological study of polar stratospheric clouds (1989–1997) from lidar measurements over Dumont d'Urville (Antarctica), *Tellus, Ser. B*, *53*, 306–321.

Simmonds, I., and K. Keay (2000), Mean Southern Hemisphere extratropical cyclone behavior in the 40-year NCEP-NCAR reanalysis, *J. Clim.*, *13*, 873–885.

Solomon, S. (1999), Stratospheric ozone depletion: A review of concepts and history, *Rev. Geophys.*, *37*, 275–316.

Stephens, G. L., et al. (2002), The CloudSat mission and the EOS constellation: A new dimension of space-based observations of clouds and precipitation, *Bull. Am. Meteorol. Soc.*, *83*, 1771–1790.

Teitelbaum, H., M. Moustaoui, and M. Fromm (2001), Exploring polar stratospheric cloud and ozone minihole formation: The primary importance of synoptic-scale flow perturbations, *J. Geophys. Res.*, *106*, 28,173–28,188.

Wang, Z., and K. Sassen (2001), Cloud type and macrophysical property retrieval using multiple remote sensors, *J. Appl. Meteorol.*, *40*, 1665–1682.

Winker, D. M., W. H. Hunt, and M. J. McGill (2007), Initial performance assessment of CALIOP, *Geophys. Res. Lett.*, *34*, L19803, doi:10.1029/2007GL030135.

World Meteorological Organization (WMO) (2007), Scientific assessment of ozone depletion: 2006, *Global Ozone Res. Monit. Proj. Rep. 50*, 572 pp., Geneva, Switzerland.

Yin, J. H. (2005), A consistent poleward shift of the storm tracks in simulations of 21st century climate, *Geophys. Res. Lett.*, *32*, L18701, doi:10.1029/2005GL023684.

L. Adhikari, T. Deshler, D. Liu, T. Parish, and Z. Wang, Department of Atmospheric Science, University of Wyoming, Laramie, WY 82072, USA. (zwang@uwyo.edu)

G. Stephens, Department of Atmospheric Science, Colorado State University, Fort Collins, CO 80523, USA.

C. Trepte and D. Winker, NASA Langley Research Center, Hampton, VA 23681, USA.

D. Vane, Jet Propulsion Laboratory, Pasadena, CA 91109, USA.